PROTONOSPHERIC-IONOSPHERIC MODELING OF VLF DUCTS

P. A. Bernhardt and C. G. Park

Radioscience Laboratory, Stanford University, Stanford, California 94305

Abstract. Numerical simulations of the ionosphere and protonosphere have been used to investigate diurnal and seasonal variations in magnetospheric plasma density enhancements capable of ducting VLF radio waves. During winter and equinoxes, VLF ducts may extend down to 300-km altitude at night but usually terminate above 1800 km during the day. In summer, ducts terminate above 1000-km altitude at all local times. The daytime flow of thermal plasma from the ionosphere into the protonosphere limits the half-life of a VLF duct to about 2 days.

Introduction

Very low frequency (VLF) wave propagation in the magnetosphere is strongly influenced by the presence of field-aligned electron density irregularities or ducts. Figure 1 illustrates schematically a ray path from a source in one hemisphere to a receiver in the conjugate hemisphere. The ray follows a snakelike path inside a duct which extends through most of the magnetosphere. Electron density gradients associated with the duct keep the ray direction and wave normal angle confined within a small cone about the field line. Rays may leave the duct and propagate in an untrapped mode to the bottom of the ionosphere. If the wave normals are nearly perpendicular to the ionosphere, signals will couple into the earth-ionosphere wave guide. By contrast, ray paths of unducted waves generally deviate outward from the starting field line, and their wave normal angle with respect to the geomagnetic field becomes so large that penetration of the conjugate ionosphere is not possible [e.g., Helliwell, 1965]. Instead, these unducted waves are magnetospherically reflected where the local lower hybrid resonance (LHR) frequency is equal to the wave frequency [Edgar, 1972, 1976]. Thus all ground-based observations of VLF waves that originate in or propagate through the magnetosphere rely on the presence of ducts.

Angerami [1970] made a detailed ray tracing analysis of whistlers received on the Ogo 3 satellite to distinguish ducted whistlers from unducted ones on the basis of their dispersion characteristics. He deduced that the ducts were ~500 km in diameter at the equator and had density enhancements of ~10-20% above the background. Edgar [1972] showed that the irregular frequency-time behavior of magnetospherically reflected whistlers received on Ogo 3 could be accurately reproduced by ray tracing calculations in a magnetosphere that contains field-aligned irregularities. Inan and Bell [1977] have suggested that the plasmapause may be used as a one-sided duct. We consider only the behavior of two-sided ducts in this paper.

Although there is strong theoretical and experimental evidence for the existence of ducts, little is known about their origin or physical properties. The coupling of wave energy into and out of a duct may depend on how low the duct extends downward in altitude and on electron density gradients near its endpoints [A. D. M. Walker, 1972, 1976; Alexander, 1971; James, 1972]. It is difficult to measure these duct parameters directly for comparisons with wave observations. It is likely that progress in this area will depend largely on accepted theories of the ionosphere and protonosphere. The aim of the present work is to predict certain aspects of duct behavior by using a coupled ionosphere-protonosphere model.

Two fundamentally different mechanisms have been suggested for the formation of VLF ducts. In the first mechanism, the localized electric field mixes tubes of plasma through $\vec{E} \times \vec{B}$ drift. Such mixing, or tube interchange motion, results in field-aligned density irregularities unless the plasma content per tube with a unit magnetic flux is uniform in space. Park and Helliwell [1971] showed that an electric field of only 0.1 mV/m in the equatorial plasma could form a whistler duct at L = 4 in about an hour. Such localized electric fields could originate in giant thunderclouds [Park and Helliwell, 1971; Park and Dejnakarintra, 1973] or in polarization charges in the ionosphere arising from unsymmetrical wind or conductivity patterns at the ends of the geomagnetic field lines [Cole, 1971]. The second mechanism involves localized enhancements in ionospheric plasma pressure which tend to increase upward plasma flux into the magnetosphere or, alternatively, decrease the magnitude of downward flux. Localized ionospheric pressure enhancements could be the result of small-scale variations in neutral atmosphere parameters or localized energetic particle precipitation from the magnetosphere. This second mechanism has not yet been studied quantitatively, but the results of the present work suggest that it is unlikely to be important except during long winter nights. The physical reason for this will become clear in a later section. However, we do not attempt in this paper to deal with the formation of ducts. Instead, we take assumed density enhancements in the protonosphere as a starting point and then examine their spatial and temporal behavior as a function of local time and season.

The next section describes the ionosphere-protonosphere model we have adopted for duct simulation, followed by a discussion of the behavior of the ionosphere-protonosphere interface.

Paper number 7A0668.

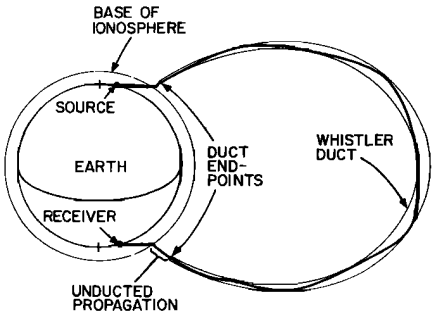

Fig. 1. Schematic of the magnetospheric propagation circuit for VLF waves. Changes in the altitude of the duct endpoints may affect the coupling between the earth-ionosphere wave guide and the magnetospheric duct.

The last two sections describe the results of duct simulation and the implications of these results for VLF wave propagation in the magnetosphere.

The Ionosphere-Protonosphere Model

The theoretical ionosphere-protonosphere model adopted for the present study is illustrated with a block diagram in Figure 2. Magnetic flux tubes extending from 100-km altitude to the equator are divided into three sections, and self-consistent plasma densities and temperatures are calculated for each section with numerical techniques.

In the lowest section, between 100 and 500 km, the ionic species considered include NO^+, O_2^+, and N_2^+ as well as O^+. (The molecular ions are included for the sake of completeness but make little difference in the results of this study.) O^+ densities are described by time-dependent continuity equations that include the effects of production, loss, ambipolar diffusion, and drift imposed by neutral air winds. In the case of molecular ions, the transport terms in the continuity equations are neglected. Electron and ion temperatures are described by a heat balance equation, including heating of the ambient electron gas by photoelectrons, heat transfer among the electron, ion, and neutral gases, and conduction along geomagnetic field lines. The neutral atmosphere model by J. C. G. Walker [1965] is combined with the exospheric temperatures and neutral wind velocities based on the work of Roble and Dickinson [1974] and Roble et al. [1977]. Further details of the model of the 100- to 500-km section can be found in Antoniadis [1977].

The middle section, extending from 500- to 3000-km altitude, is assumed to be populated by a mixture of O^+, H^+, and electrons. O^+ ions are assumed to be in diffusive equilibrium, while the H^+ density profile is described by a time-dependent continuity equation that includes the effects of the charge exchange reaction $O + H^+ \rightleftarrows O^+ + H$, as well as field aligned diffusion through the ambient O^+ ions. Electron temperatures in this section are calculated from a heat equation assuming constant heat flow throughout the entire altitude range. O^+ and H^+ temperatures are assumed to be equal and are calculated from electron and neutral temperatures with expressions developed previously [e.g. Banks and Kockarts, 1973; Chap. 23]. A detailed description of the model between 500 and 3000 km can be found in Park and Banks [1974, 1975].

The region between 3000-km altitude and the geomagnetic equator is treated like a finite reservoir of H^+ and electrons. The plasma is assumed to be in diffusive equilbrium at all times, so that the density at any point along the flux tube is simply proportional to the tube plasma content. The temperature profiles for this uppermost section are not calculated. Instead, this section is treated like a heat reservoir of infinite capacity, capable of supplying whatever heat flux is consistent with the calculated temperature profiles at lower altitudes.

Calculations of plasma densities and temperatures below 3000 km require numerical solutions of the above-mentioned equations subject to the following boundary conditions. At the 3000-km boundary we assume an initial plasma density as well as the plasma content in the reservoir above that altitude. As time progresses, calculated fluxes into and out of the reservoir give temporal variations of the plasma content and therefore of the density at 3000 km. At 100 km we assume a state of chemical equilibrium, and at the 500-km boundary we require that plasma densities and temperatures be continuous. A detailed description of the coupled ionosphere-protonosphere model can be found in Bernhardt [1976].

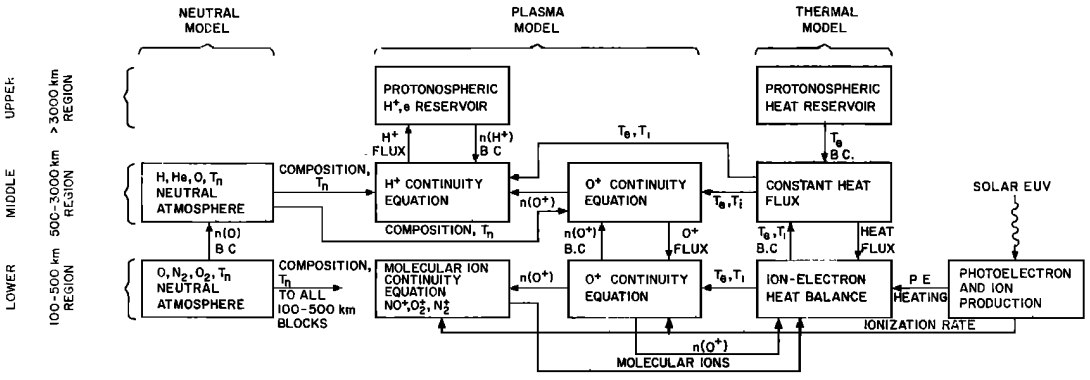

Fig. 2. Block diagram of the protonospheric-ionospheric model.

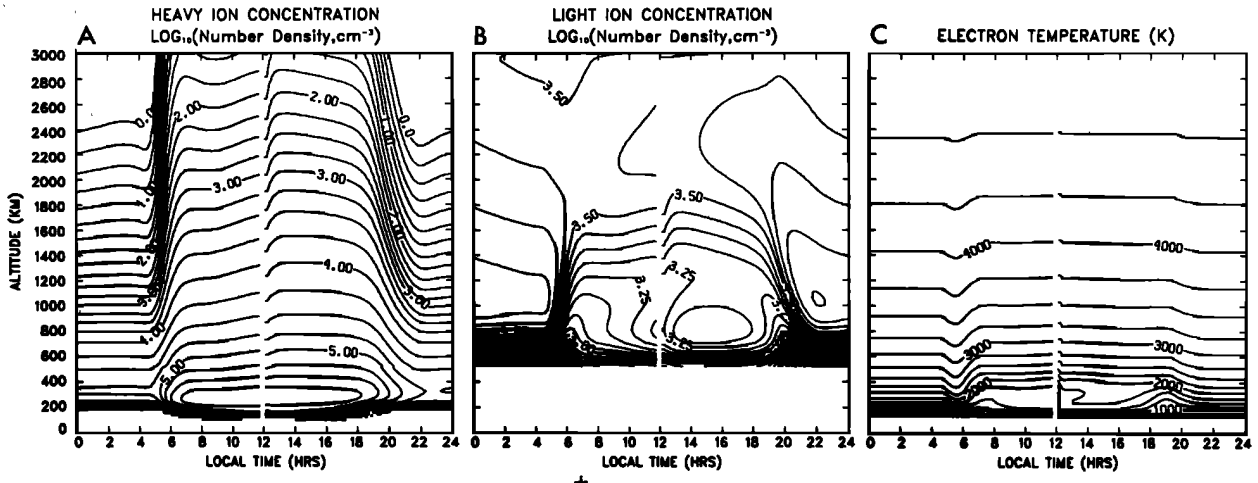

Fig. 3. Diurnal behavior of the (a) O^+ concentration plus molecular ion concentration, (b) H^+ concentration, and (c) electron temperature during equinox with an initial protonospheric concentration of 3000 cm^{-3} at 3000-km altitude.

Behavior of the Ionosphere-Protonosphere Interface

In this section we examine some aspects of the coupled ionosphere-protonosphere system that are relevant to the study of ducts. Sample calculations were made for 60° invariant latitude (L = 4) and 49° geographic latitude at the foot of the field line, a combination appropriate for eastern North America. No electric field was assumed to exist, so the plasma would simply corotate with the earth. Time-dependent solutions were obtained for complete diurnal cycles during equinox, summer, and winter so that diurnal and seasonal variations in coupling fluxes and the O^+-H^+ transition height can be examined.

The contour maps of Figure 3 show calculated heavy (O^+, O_2^+, N_2^+, and NO^+) and light (H^+) ion concentrations and electron temperatures at equinox. The calculations were initiated with steady state solutions at 1200 LT. After the steady state solutions are formed, the plasma and thermal continuities equations are solved with the inclusion of the time-varying terms. The transition from steady state solutions to time-dependent solutions occurs in less than 30 min. The solution is carried out over a 24-hour period. A relatively full protonosphere was assumed with an initial density of 3000 cm^{-3} at 3000 km and an initial tube content of 3×10^{13} el between 3000 km and the magnetic equator [see Park, 1974]. The flux tube has a 1-cm^2 cross-sectional area at 500-km altitude. In Figure 3a, molecular ions are important only during sunlight hours (0600-2000 LT) and below 200 km. The general behavior of the ionosphere is in good agreement with observations [Titheridge, 1976] as well as the results of previous theoretical calculations [Roble, 1975; Murphy et al., 1976].

Figure 4 shows two fundamentally different ion density profiles. Figure 4a illustrates a nighttime situation where the O^+ layer is maintained by the charge exchange reaction of H^+ ions ($H^+ + O \rightarrow O^+ + H$) that diffuse downward from the protonosphere. Both O^+ and H^+ profiles are close to diffusive equilibrium distributions. By contrast, Figure 4b shows dynamic daytime profiles that depart sharply from diffusive equilibrium. Large upward fluxes of H^+ significantly deplete the H^+ density and

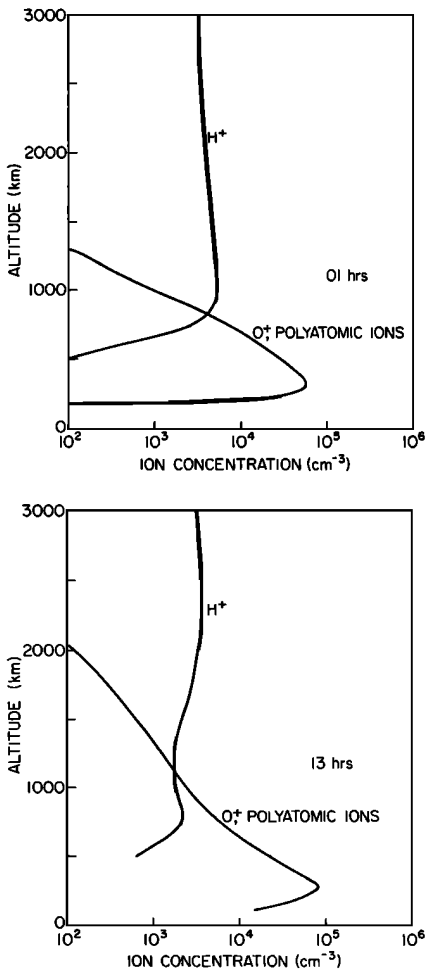

Fig. 4. Profiles of the O^+ plus molecular ions and H^+ ion layers during equinox at (a) nighttime and (b) daytime.

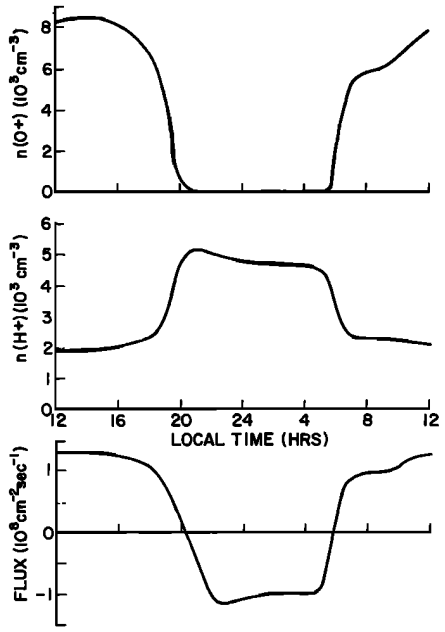

Fig. 5. Variation of O^+ and H^+ ion concentrations and plasma fluxes at 1400-km altitude throughout the equinox day. A full protonosphere with an H^+ concentration of 3000 cm^{-3} at 3000 km is used in the simulation.

raise the $O^+ - H^+$ transition height. Such effects have been discussed by a number of authors including Park and Banks [1975] and Murphy et al. [1976]. An important point to be noted here is that they can occur even when the protonosphere has relatively high densities that are typical of the plasmasphere. Figure 5 shows diurnal variations of O^+ density, H^+ density, and H^+ flux at 1400-km altitude. Dramatic composition changes and flux reversals occur near sunrise and sunset.

If the same calculations described above are repeated with lower initial protonospheric densities, the results remain essentially unchanged except for the fact that the daytime depletion of H^+ in the topside ionosphere and consequent raising of the transition height are more pronounced. For example, a reduction in the 3000-km density from 3000 cm^{-3} to 1000 cm^{-3} causes the daytime transition height to increase from 1200 km to 2000 km. The daytime O^+ layer, produced by photo-ionization, is not significantly affected by density changes in the overlying protonosphere (also see Park and Banks [1975]). At night, both O^+ and H^+ densities are reduced by a factor of approximately 3, and no significant change in the transition height results.

Returning to Figure 3a, we note that ionospheric densities decrease rapidly after sunset but become stabilized around 2200 LT and remain essentially unchanged until sunrise near 0500 LT. The stable nighttime ionosphere is maintained by downward flux from the overlying protonosphere. This nighttime behavior changes with the season as sunlight conditions and neutral air wind patterns change. In the winter the stable nighttime ionosphere persists for longer periods, but its qualitative behavior is similar to that near equinoxes. However, the summer night ionosphere is significantly different, as shown in Figure 6. The format of Figure 6 is identical with that of Figure 3 except that the calculations were initiated at 1800 LT instead of 1200 LT. The summer ionosphere decays much more slowly after sunset owing both to slower rates of change in the solar zenith angle and to earlier reversal in the neutral wind direction from poleward to equatorward [e.g., Antoniadis, 1976]. This equatorward shift in wind direction lifts the ionosphere to higher altitudes where the loss rates are smaller. Thus the summer night ionosphere does not reach low density levels where it can be strongly influenced by downward fluxes from the protonosphere. Figure 7 shows diurnal variations of O^+ density, H^+ density, and H^+ flux at 1400 km in the same format as Figure 4.

Modeling of Enhancement Ducts

In this section we examine the spatial and temporal behavior of ducts. We consider a meridional plane with a horizontal plasma den-

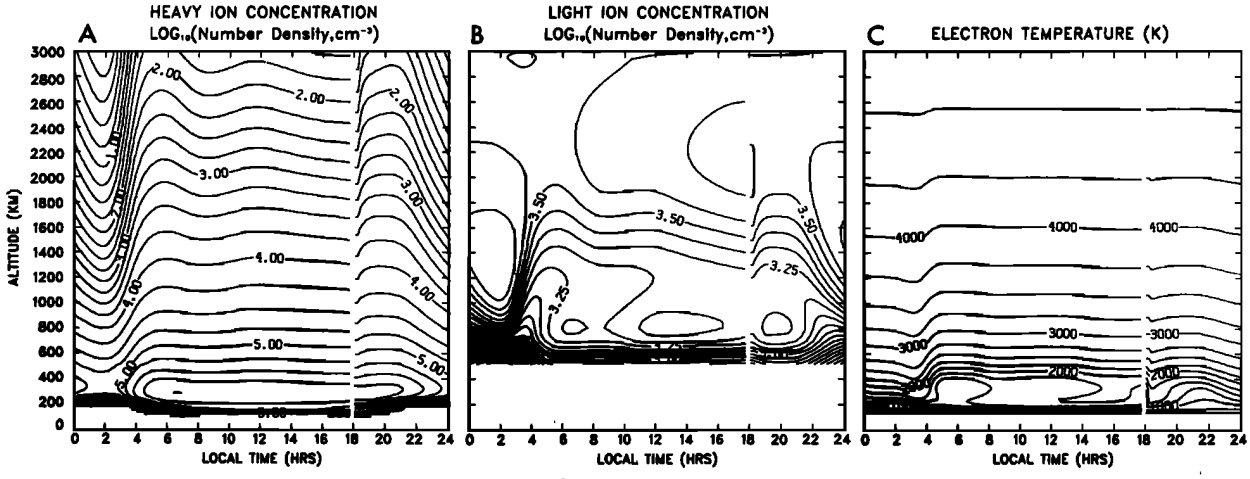

Fig. 6. Diurnal behavior of the (a) O^+ concentration plus molecular ion concentration, (b) H^+ ion concentration, and (c) electron temperature during summer with an initial protonospheric concentration of 3000 cm^{-3} at 3000 km is used in the simulation.

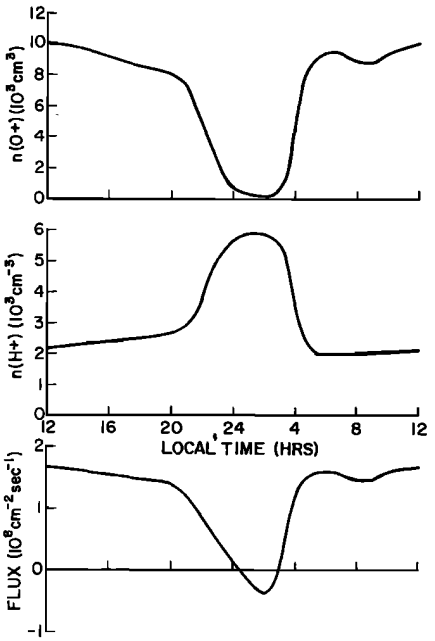

Fig. 7. Variation of O^+ and H^+ ion concentrations and plasma fluxes at 1400-km altitude throughout the summer day. A full protonosphere with an H^+ concentration of 3000 cm^{-3} at 3000 km is used in the simulation.

sity variation specified at 3000-km altitude as an initial boundary condition. An enhancement duct is described by

$$n_e\Big|_{3000\ km} = 3 \times 10^3[1 + \phi \exp(-x^2/2\sigma^2)]\ cm^{-3}$$

where n_e is electron concentration, x is horizontal distance measured in km from the center of the duct at 3000 km altitude, ϕ is the enhancement factor = 15%, and σ is the duct radius = 20 km. The duct is centered on an L = 4 field line, which intersects the earth's surface at 49° geographic latitude (appropriate for eastern North America).

The ionosphere-protonosphere model described earlier was used to study how the duct extends down to lower altitudes and how its behavior depends on local time and season. Time-dependent calculations were performed for a number of neighboring field lines in order to see the evolution of the duct shape in two dimensions. Figure 8 shows the results of the duct simulation for equinox with a sequence of meridional plane contour maps at four different local times. The calculations were initiated at 1100 LT, but the results are presented only after 1200 LT after complete transition from a steady state to a time-varying simulation. The dashed lines represent the magnetic field line passing through the center of the duct. It is apparent that the duct termination altitude (arbitrarily defined as the altitude where the enhancement factor is reduced to one tenth of the value at 3000 km) is a strong function of local time and ranges from ~300 km at midnight to ~1800 km at noon.

Figure 9 shows the enhancement factor at the center of the duct as a function of altitude at noon and midnight. The enhancement factor decreases sharply below 2500 km at noon, but at midnight it remains constant down to ~1200 km and then increases to a slight maximum near 400 km before dropping to zero at ~200 km.

The diurnal variation of the duct termination height can be understood in terms of the ionization source for the ionosphere discussed in the previous section. During daylight hours, photoionization produces a dense ionosphere sending large fluxes of plasma into the overlying protonosphere. The ionospheric O^+ densities are not affected by small changes in protonospheric densities, and a duct would effectively terminate at the $O^+ - H^+$ transition height. At night,

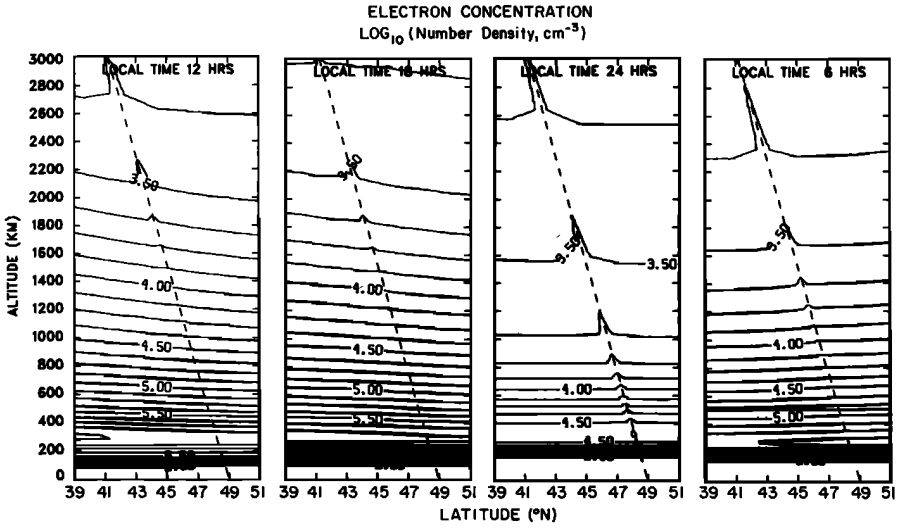

Fig. 8. Variations in the equinox plasmasphere containing a 15% enhancement duct at L = 4. The field line is indicated by the dashed line. Perturbations in the contour lines indicate the presence of an enhanced tube of plasma.

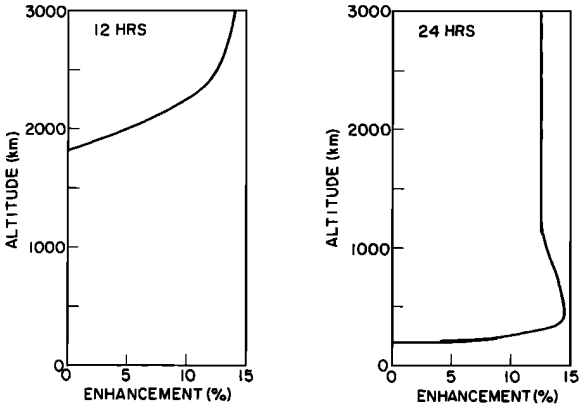

Fig. 9. Profiles of equinox duct endpoints at noon and midnight.

when the ionosphere is maintained by a downward flux from the protonosphere, the flux is directly proportional to the protonospheric density, so that small density variations in the protonosphere are reflected all the way down through the ionosphere. This is clearly illustrated in Figure 10, where the duct termination height is plotted as a function of local time. Also plotted in the figure is the $O^+ - H^+$ transition height. When the ionosphere is under solar control, the duct terminates at the transition height, but extends to lower altitudes as the nighttime protonosphere becomes an important source of ionization.

When the ionosphere is sunlit, upward plasma flow is insensitive to the plasma density in the overlying protonosphere (also pointed out by Murphy et al. [1976]). For example, if the protonospheric density is increased by 15%, the upward flux is decreased by only 2%. Thus the filling flux is nearly uniform and tends to smear out any spatial density gradients in the protonosphere. The result is to shorten the duct lifetime. By contrast, downward plasma flux at night is proportional to the protonospheric density so that the duct enhancement factor remains unaffected. Figure 11 shows a plot of the duct enhancement factor at 3000-km altitude as a function of time. The initial condition was 15% enhancement at 1100 LT, but the plot begins at 1200 LT to allow for a short transition from steady state to time-dependent solutions (see Figure 3). It can be seen in Figure 11 that the duct enhancement factor decreases during daylight hours but remains approximately constant at night. The half-life of the duct due to this process is estimated to be 2.3 days.

The foregoing discussion applies to equinox conditions. The behavior of the duct depends on the season as the nature of protonosphere-ionosphere coupling changes with season. Figures 12 and 13 show the duct behavior in winter and summer, respectively, in the same format as Figure 9. The winter duct terminates at the $O^+ - H^+$ transition height during the day but extends close to the bottom of the ionosphere at night. The winter behavior is similar to the equinox behavior discussed above, except that the night is longer in winter. In the summer, however, the duct endpoint remains high at all local times. This can be understood in terms of the behavior of the summer night ionosphere, discussed in the previous section. In the summer the ionosphere decays very slowly after sunset, and the night is not long enough to allow the densities to reach levels where the protonospheric flux plays an important role in their maintenance. Thus the protonosphere never exerts much influence over the underlying ionosphere throughout the night. Figure 14 shows a plot of the duct termination altitude as a function of local time in the summer. The duct never extends below 1000 km even at night, in sharp contrast to the winter and equinox behavior.

Discussion and Concluding Remarks

We have used an ionosphere-protonosphere model to study certain properties of VLF ducts. In particular, we have found that the height of the duct endpoint depends strongly on local time and season. This is important for magnetospheric VLF studies for several reasons. If a duct terminates at a high altitude, much of the propagation path may lie in an unducted region resulting in spreading of waves in the topside ionosphere. When these waves are reflected (or refracted) upward, they may couple into neighboring ducts and return to the conjugate hemisphere, thus giving rise to mixed path propagation

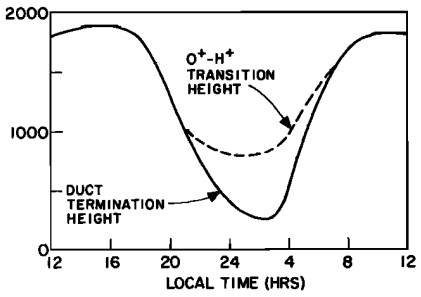

Fig. 10. Variation of the duct termination height and the O^+-H^+ transition height throughout the equinox day. The two heights coincide during the daytime.

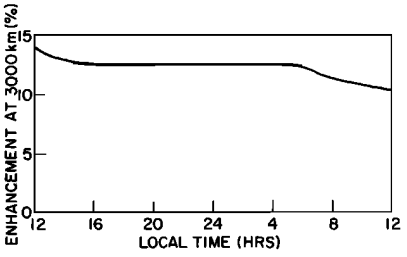

Fig. 11. Decay of the enhancement level at 3000 km during equinox. The enhancement level drops steadily during the daytime. The half-life of the duct is 2.3 days.

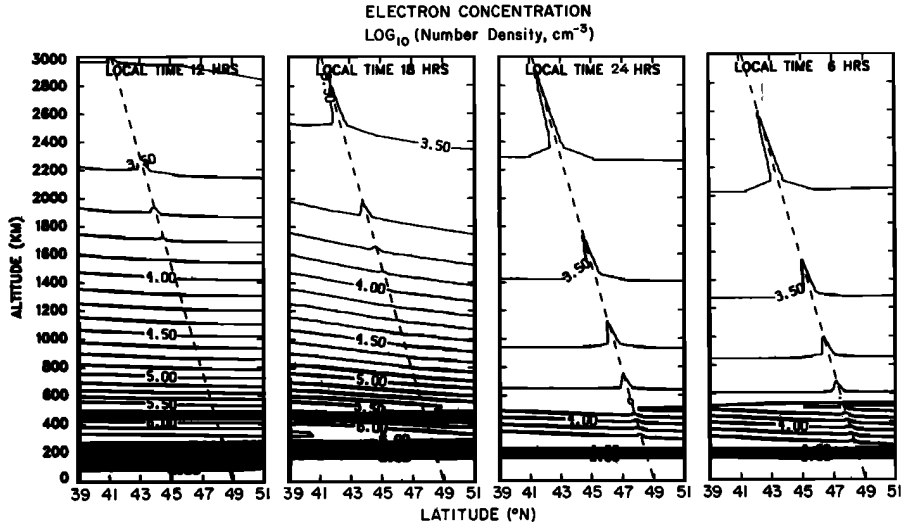

Fig. 12. Variations in the winter plasmasphere containing a 15% enhancement duct at L = 4.

[Helliwell, 1965]. The waves that leave the duct at high altitudes may deviate significantly from the duct field line before emerging into the earth-ionosphere wave guide. If ground-based direction finders are used to locate the duct, corrections must be made to the apparent duct exit point. By contrast, a duct that extends down to the bottom of the ionosphere may keep the waves trapped on a fixed field line. Coupling of upgoing waves into a duct would similarly depend on the height of the duct endpoint.

The efficiency of signal coupling between the earth-ionosphere waveguide and magnetospheric ducts is of importance to studies of VLF amplification in the magnetosphere. Measurements indicate as much as 30 dB amplification by wave-particle interaction in the magnetosphere [Helliwell and Katsufrakis, 1974]. The overall efficiency of the 'magnetospheric amplifier' is a function of the coupling into and out of the ducts. These problems are being investigated by using a combination of the duct simulation program discussed here and a VLF ray tracing program.

In this paper we ignored the effects of electric fields on ducts. As was mentioned earlier, it is likely that small-scale electric fields are responsible for the formation of most ducts. If these fields persist after the ducts are formed, the resulting flux tube interchange motion would continuously change the duct shape and size [Park and Helliwell, 1971]. Enhanced wave activity inside a duct could conceivably modify the electric field by modulating the E region conductivity through particle precipitation.

Another effect not considered in this paper is the precipitation of low-energy particles that are deposited in the F region. These particles

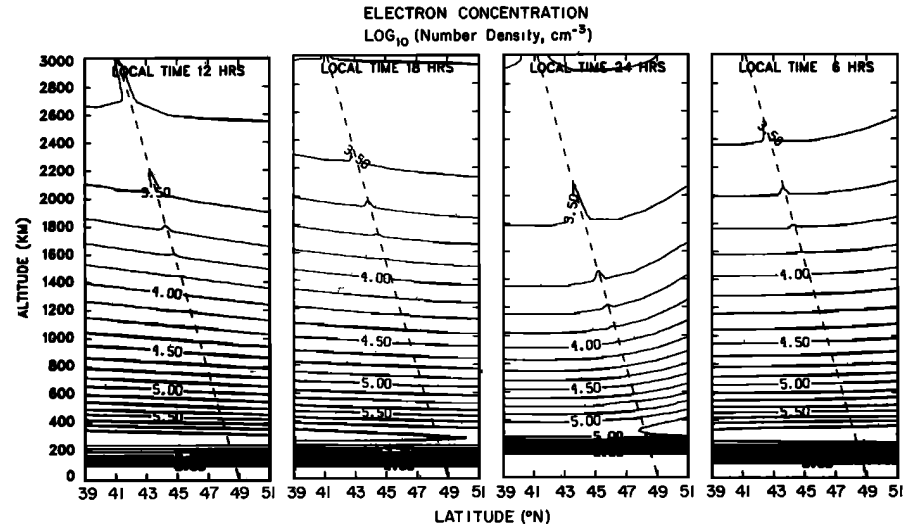

Fig. 13. Variations in the summer plasmasphere containing a 15% enhancement duct at

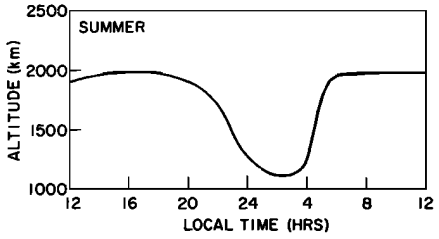

Fig. 14. Temporal variation of the duct termination height during summer. The duct endpoint height is the same as the $O^+ - H^+$ transition height.

may provide a significant source of ionization for the nighttime F layer, but their effects on ducts depend on the spatial distribution as well as on the magnitude of precipitation flux. In the case of uniform precipitation, ducts are not expected to extend as low as the results of the previous section indicated. This is because corpuscular ionization makes the ionosphere less dependent on thermal plasma flow from the protonosphere and therefore makes the nighttime ionosphere behave more like a daytime ionosphere. On the other hand, if enhanced wave activity inside a duct produced a local enhancement in precipitation flux through wave-particle interactions, the resulting effects on ducts would be quite different. First, the duct enhancement factor would be increased at ionospheric heights due to corpuscular ionization, and second, the resulting increase in ionospheric pressure would reduce the nighttime downward flux thus increasing duct enhancement factor in the protonosphere. The latter may be an important positive feedback mechanism by which ducts can grow at night. Particle precipitation is not expected to be important during daytime when photo-ionization is the dominant plasma production mechanism.

Acknowledgements. The authors would like to thank R. A. Helliwell, D. L. Carpenter, and T. F. Bell for many useful discussions during the course of this work. This research was supported in part by the Office of Naval Research under grant N00014-76-C-0689 and in part by the National Science Foundation, Atmospheric Sciences Section, under grant ATM-74-20084. Acknowledgement is made to the National Center for Atmospheric Research, which is sponsored by the National Science Foundation, for the computing time used in this research.

The Editor thanks J. C. Cerisier and A. D. M. Walker for their assistance in evaluating this paper.

References

Alexander, P. H., Computation of ray paths for very low frequency radio waves propagating through the magnetospheric plasma, Ph. D. thesis, Univ. of Southampton, England, 1971.

Angerami, J. J., Whistler duct properties deduced from VLF observations with the Ogo 3 satellite near the magnetic equator, J. Geophys. Res., 75, 6115, 1970.

Antoniadis, D. A., Thermospheric winds and exospheric temperatures from incoherent scatter radar measurements in four seasons, J. Atmos. Terr. Phys., 38, 187, 1976.

Antoniadis, D. A., Determination of thermospheric quantities from simple ionospheric observations using numerical simulation, J. Atmos. Terr. Phys., 39, 531, 1977.

Banks, P. M., and G. Kockarts, Aeronomy, vols. A and B., Academic, New York, 1973.

Bernhardt, P. A., The response of the ionosphere to the injection of chemically reactive vapors, Tech. Rept. 17, SU-SEL-76-009, Stanford Univ., Stanford, Calif., 1976.

Cole, K. D., Formation of field aligned irregularities in the magnetosphere, J. Atmos. Terr. Phys., 33, 741, 1971.

Edgar, B. C., The structure of the magnetosphere as deduced from magnetospherically reflected whistlers, Ph. D. thesis, Stanford Univ., Stanford, Calif., 1972.

Edgar, B. C., The upper and lower frequency cutoffs of magnetospherically reflected whistlers, J. Geophys. Res., 81, 205, 1976.

Helliwell, R. A., Whistlers and Related Ionospheric Phenomena, Stanford University Press, Stanford, Calif., 1965.

Helliwell, R. A., and J. P. Katsufrakis, VLF wave injection into the magnetosphere from Siple Station, Antarctica, J. Geophys. Res., 79, 2511, 1974.

Inan, U. S. and T. F. Bell, The plasmapause as a VLF waveguide, J. Geophys. Res., 82, 2819, 1977.

James, H. G., Refraction of whistler mode waves by large scale gradients in the middle latitude ionosphere, Ann. Geophys., 28, 301, 1972.

Murphy, J. A., G. J. Bailey, and R. J. Moffett, Calculated daily variations of O^+ and H^+ at mid-latitudes, I, Protonospheric replenishment and F-region behavior at sunspot minimum, J. Atmos. Terr. Phys., 38, 351, 1976.

Park, C. G., Some features of plasma distribution in the plasmasphere deduced from Antarctic whistlers, J. Geophys. Res., 79, 169, 1974.

Park, C. G. and P. M. Banks, Influence of the thermal plasma flow on the mid-latitude F_2 layer: Effects of electric fields and neutral winds in the plasmasphere, J. Geophys. Res., 79, 4661, 1974.

Park, C. G. and P. M. Banks, Influence of thermal plasma flow on the daytime F_2 layer, J. Geophys. Res., 80, 2819, 1975.

Park, C. G. and M. Dejnakarintra, Penetration of thundercloud electric fields into the ionosphere and the magnetosphere, 1, Middle and subauroral latitudes, J. Geophys. Res., 78, 6623, 1973.

Park, C. G. and R. A. Helliwell, The formation by electric fields of field-aligned irregularities in the magnetosphere, Radio Sci., 6, 299, 1971.

Roble, R. G., The calculated and observed diurnal variation of the ionosphere over Millstone Hill on March 23-24, 1970, Planet. Space Sci., 23, 1017, 1975.

Roble, R. G. and R. D. Dickinson, The effect of displaced geomagnetic and geographic roles on the thermospheric neutral winds, Planet. Space Sci., 22, 623, 1974.

Roble, R. E., J. E. Salah, and B. A. Emery, The seasonal variation of the diurnal thermo-

spheric winds over Millstone Hill during solar maximum, J. Atmos. Terr. Phys., in press, 1977.
Titheridge, J. E., Plasmapause effects in the topside ionosphere, J. Geophys. Res., 81, 3227, 1976.
Walker, A. D. M., The propagation of very low frequency waves in ducts in the magnetosphere, Proc. Roy. Soc. London, Ser. A, 321, 69, 1971.
Walker, A. D. M., The theory of whistler propagation, Rev. Geophys. Space Phys., 14, 629, 1976.
Walker, J. C. G., Analytic representation of upper atmosphere densities based on Jacchia's static diffusion models, J. Atmos. Sci., 22, 462, 1965.

(Received April 28, 1977;
accepted July 13, 1977.)